Mon. Not. R. Astron. Soc. **368,** 1101–1109 (2006) doi:10.1111/j.1365-2966.2006.10188.x

GRB 050505: a high-redshift burst discovered by *Swift*

C. P. Hurkett,[1⋆] J. P. Osborne,[1] K. L. Page,[1] E. Rol,[1] M. R. Goad,[1] P. T. O'Brien,[1] A. Beardmore,[1] O. Godet,[1] D. N. Burrows,[2] N. R. Tanvir,[3] A. Levan,[3] B. Zhang,[4] D. Malesani,[5] J. E. Hill,[6,7] J. A. Kennea,[2] R. Chapman,[3] V. La Parola,[8] M. Perri,[9] P. Romano,[10] R. Smith[11] and N. Gehrels[6]

[1]*X-ray & Observational Astronomy Group, Department of Physics & Astronomy, University of Leicester, Leicester LE1 7RH*
[2]*Department of Astronomy & Astrophysics, Penn State University, University Park, PA 16802, USA*
[3]*Centre for Astrophysics Research, University of Hertfordshire, College Lane, Hatfield, AL10 9AB*
[4]*Department of Physics, University of Nevada, Las Vegas, NV 89154, USA*
[5]*International School for Advanced Studies (SISSA-ISAS), via Beirut 2-4, 34014 Trieste, Italy*
[6]*NASA/Goddard Space Flight Center, Greenbelt, Maryland, MD 20771, USA*
[7]*Universities Space Research Association, 10211 Wincopin Circle, Suite 500, Columbia, MD 21044-3432, USA*
[8]*INAF – Istituto di Astrofisica Spaziale e Fisica Cosmica, Sezione di Palermo, Via La Malfa 153, I-90146 Palermo, Italy*
[9]*ASI Science Data Center, Via Galileo Galilei, I-00044 Frascati, Italy*
[10]*INAF – Osservatorio Astronomico di Brera, Via Bianchi 46, 1-23807 Merate, Italy*
[11]*Astrophysics Research Institute, Liverpool John Moores University, Twelve Quays House, Birkenhead CH41 1LD*

Accepted 2006 February 9. Received 2006 January 31; in original form 2005 November 25

ABSTRACT

We report the discovery and subsequent multiwavelength afterglow behaviour of the high-redshift ($z = 4.27$) Gamma Ray Burst (GRB) 050505. This burst is the third most-distant burst, measured by spectroscopic redshift, discovered after GRB 000131 ($z = 4.50$) and GRB 050904 ($z = 6.29$). GRB 050505 is a long GRB with a multipeaked γ-ray light curve, with a duration of $T_{90} = 63 \pm 2$ s and an inferred isotropic release in γ-rays of $\sim 4.44 \times 10^{53}$ erg in the 1–10^4 keV rest-frame energy range. The *Swift* X-Ray Telescope followed the afterglow for 14 d, detecting two breaks in the light curve at $7.4^{+1.5}_{-1.5}$ and $58.0^{+9.9}_{-15.4}$ ks after the burst trigger. The power-law decay slopes before, between and after these breaks were $0.25^{+0.16}_{-0.17}$, $1.17^{+0.08}_{-0.09}$ and $1.97^{+0.27}_{-0.28}$, respectively. The light curve can also be fitted with a 'smoothly broken' power-law model with a break observed at $\sim T + 18.5$ ks, with decay slopes of $\sim$0.4 and $\sim$1.8, before and after the break, respectively. The X-ray afterglow shows no spectral variation over the course of the *Swift* observations, being well fitted with a single power law of photon index $\sim$1.90. This behaviour is expected for the cessation of the continued energization of the interstellar medium shock, followed by a break caused by a jet, either uniform or structured. Neither break is consistent with a cooling break. The spectral energy distribution, indeed, shows the cooling frequency to be below the X-ray but above the optical frequencies. The optical–X-ray spectrum also shows that there is significant X-ray absorption in excess of that due to our Galaxy but very little optical–ultraviolet extinction, with $E(B - V) \approx 0.10$ for a Small Magellanic Cloud like extinction curve.

Key words: galaxies: high-redshift – galaxies: ISM – gamma-rays: bursts – gamma-rays: observations.

1 INTRODUCTION

Gamma Ray Bursts (GRBs) are expected to be visible over a large range of redshifts with a potential upper limit of $z \sim 15$–20 (Lamb & Reichart 2000). The lowest recorded GRB redshift to date is GRB 980425 with $z = 0.0085 \pm 0.0002$ (Tinney et al. 1998), whilst the highest is GRB 050904 at $z = 6.29 \pm 0.01$ (Kawai et al. 2005)[1] Bursts at high redshifts are potentially important, since they can be

⋆E-mail: cph9@star.le.ac.uk

[1]We also note that a photometric redshift of $\sim$6.6 has been reported for GRB 060116 (Grazian et al. 2006; Malesani et al. 2006), but this has yet to be confirmed spectroscopically.

powerful probes of the early Universe. Long-duration bursts ($T_{90} \geqslant 2$ s) are likely caused by the core-collapse of a massive star (Hjorth et al. 2003; Stanek et al. 2003), linking these bursts directly to contemporary star formation. In addition, high-redshift GRBs allow us to probe the intervening matter between the observer and GRB, and particularly the conditions of their host galaxies (e.g. Vreeswijk et al. 2004).

So far, only ∼50 bursts have a firm redshift determination, mostly obtained through the spectroscopy of their optical afterglow. The record holder is GRB 050904, see Watson et al. (2005), Cusumano et al. (2005) and Tagliaferri et al. (2005), for more details. Previously, the highest-redshift burst was GRB 000131 (Andersen et al. 2000). Unfortunately, *BATSE* detected GRB 000131 during a partial data gap (Kippen 2000), so its position was not localized until 56 h after the trigger, thus, its early-time behaviour is unknown. No breaks were directly observed in the light curve for GRB 000131 but, based on the spectral index, an upper limit on the jet break time of <3.5 d has been hypothesized (Andersen et al. 2000). In contrast, the rapid position dissemination for GRB 050505 allowed a rapid redshift determination, and its automated follow-up program provided a well-covered X-ray afterglow light curve. Here, we present the results from *Swift* (Gehrels et al. 2004) on GRB 050505. Two breaks were detected in the X-ray light curve, the first of which we consider to be due to the cessation of continued energization of the interstellar medium (ISM) shock and the second is a jet break, caused by either a structured or uniform jet. Both the breaks are inconsistent with a cooling break passing through the X-ray band (see Section 4.1).

2 *SWIFT* OBSERVATIONS OF GRB 050505

At 23:22:21 UT on 2005 May 5, the *Swift* Burst Alert Telescope (BAT; Barthelmy et al. 2005), triggered and located GRB 050505 on-board (trigger ID 117504; Hurkett et al. 2005). The BAT mask-weighted light curve (see Fig. 1) shows a multipeaked structure with a T_{90}[2] (15–350 keV) of 63 ± 2 s. The initial peak began ∼15 s before the trigger and extended to 10 s after the trigger. There were three further short spikes with peaks at $T + 22.3$, $T + 30.4$ and $T + 50.4$ s, where T is the trigger time.

The T_{90} observed 15–150 keV BAT spectrum was adequately fitted by a single power law with a photon index $= 1.56 \pm 0.12$ (with χ^2/d.o.f.$= 48/56$) and a mean flux over T_{90} of $(6.44^{+0.42}_{-1.54}) \times 10^{-8}$ erg cm^{-2} s^{-1} in the 15–350 keV range and $(3.76^{+0.21}_{-0.69}) \times 10^{-8}$ erg cm^{-2} s^{-1} in the 15–150 keV range. All errors in this paper are quoted at 90 per cent confidence level, unless otherwise stated. Whilst fitting a cut-off power law does not give a significantly better fit (χ^2/d.o.f.$=$ 45/55), it does provide us with an indication of the $E_{\rm peak}$ for this burst. We find a photon index $= 1.02^{+0.51}_{-0.57}$ and a lower limit of $E_{\rm peak,obs} > 52$ keV (at the 90 per cent confidence level).

The burst was detected in each of the four standard BAT energy bands and had a ratio of fluence in the 50–100 keV band to that in the 25–50 keV band of 1.37 ± 0.14, close to the mean ratio of the *BATSE* catalogue.[3] The total fluence in the 15–350 keV band is $(4.1 \pm 0.4) \times 10^{-6}$ erg cm^{-2} (Hullinger et al. 2005), which is slightly higher than the average fluence detected to date by *Swift*.

Swift executed an automated slew to the BAT position and the X-Ray Telescope (XRT; Burrows et al. 2005), began taking data at 00:09:23 UT on 2005 May 6, ∼47 min after the burst trigger. The delay in the spacecraft slew was due to an Earth limb observing constraint. The XRT was in the Auto state, where autonomous data mode switching was enabled, but the on-board software did not automatically locate a position due to low source brightness. Ground processing revealed an uncatalogued X-ray source within the BAT error circle located at RA = 09:27:03.2, Dec. = +30:16:21.5 (J2000) with an estimated uncertainty of 6 arcsec radius (90 per cent containment; Kennea et al. 2005). Updating the XRT boresight, Moretti et al. (2005) have corrected this position to RA = 09:27:3.16, Dec. = +30:16:22.7 with an estimated uncertainty of 3.2 arcsec (also 90 per cent containment). No data were obtained in the Window Timing mode due to the delayed slew, since this mode is only used for sources brighter than 1 mCrab.

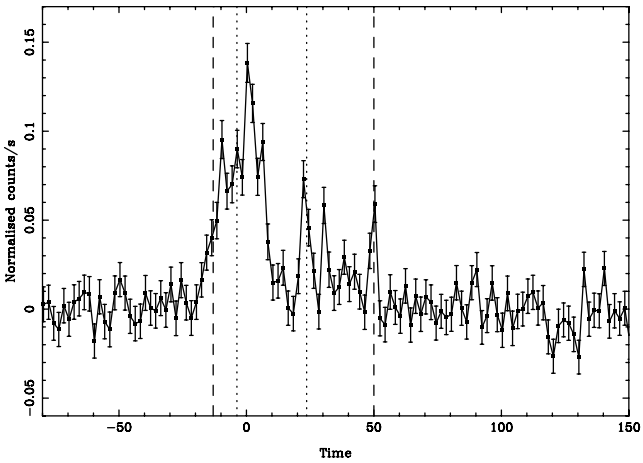

Figure 1. The BAT mask-weighted light curve (15–350 keV), where $T = 0$ is the trigger time. The dashed lines indicate the T_{90} interval and the dotted lines indicate the T_{50} interval.

The observations continued over the next 14 d, though the X-ray afterglow was not detected after the sixth day. Co-adding the final 8 d of observations produced a total of 58 ks of data providing an upper limit of $\sim 3.5 \times 10^{-4}$ counts s^{-1}, consistent with the extrapolated decay (see Section 2.1).

The *Swift* UltraViolet/Optical Telescope (UVOT; Roming et al. 2005), observed the field starting at 00:09:08 UT on 2005 May 6, ∼47 min after the burst trigger. The initial data were limited to one 100-s exposure in each of the four filters. No new sources were found in the XRT error circle to limiting magnitudes (5σ in 6-arcsec-radius apertures) of $V > 17.7$, $U > 18.4$, *UVW1* > 18.9 and *UVM2* > 19.7. Additional co-added, deeper exposures (∼2000 s) with the UVOT also failed to detect an optical counterpart at the location of the GRB (Rosen et al. 2005a,b). The deeper exposure in V placed a limiting magnitude for the source at >20.35 (3σ confidence level) for a total exposure of 2527 s co-added from a series of short exposures over the time-span of 2807 to 28 543 s after the trigger. Due to the delayed slew of the satellite, we cannot confirm whether this burst was intrinsically subluminous or had faded below the detection level of the UVOT. However, the optical counterpart for this burst was detected by several other facilities (see Table 2), which argues for the case that it was merely too faint to be detected by the UVOT ∼47 min postburst.

2.1 X-ray light curve and spectral analysis

In the Photon Counting mode, the XRT suffers from pile-up when the count-rate is $\geqslant 0.8$ counts s^{-1} (Vaughan et al. 2005). To counter

[2]The time during which 90 per cent of the counts are accumulated.
[3]http://cossc.gsfc.nasa.gov/docs/cgro/batse/4Bcatalog/index.html.

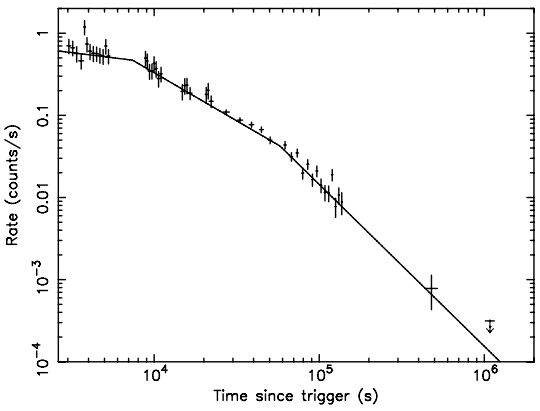

Figure 2. The 0.3–10.0 keV X-ray light curve of GRB 050505 fitted to a doubly broken power law (see Section 2.1). The first decay slope, $\alpha_1 = 0.25^{+0.16}_{-0.17}$, which breaks sharply at $t_1 = 7.4^{+1.5}_{-1.5}$ ks (observer's frame) to the second decay slope of $\alpha_2 = 1.17^{+0.08}_{-0.09}$. A second break occurs at $t_2 = 58^{+9.9}_{-15.4}$ ks into a third decay slope of $\alpha_3 = 1.97^{+0.27}_{-0.28}$. The final point on the light curve is the 3σ upper limit to the detection of the afterglow at that time.

the effects of pile-up, we extracted a series of grade 0–12 spectra from the first 23 ks of data, using annuli of varying inner radii. These background-corrected spectra were then fitted in XSPEC with an absorbed power law. We deem the point at which pile-up no longer affects our results to be when the power-law index does not vary, when the inner radius of the annulus is increased. For GRB 050505, this occurred when we excluded the inner 8 pixels (radius). Data after $T + 23$ ks were not piled up and therefore required no correction.

The X-ray light curve of GRB 050505 is shown in Figs 2 and 3, with observations starting at $T + 3$ ks after the trigger time and extending to $T + 1.05 \times 10^3$ ks. We characterize the behaviour of the XRT flux in terms of the standard power-law indices $f \propto \nu^{-\beta} t^{-\alpha}$. Thus, a series of power-law models were fitted to the light curve data. The simplest model considered was a single power law of decay index α. This model was rejected for GRB 050505 as it gave an unacceptable value of χ^2/d.o.f.= 122.5/46.

'Broken' and 'doubly broken' power laws were also fitted to the data. These models consist of two or three (respectively) power-law sections whose slopes join but change instantaneously from α_i to α_{i+1} at the break times. A 'broken' power-law model is also a poor description of the light curve ($\alpha_1 = 0.90^{+0.05}_{-0.05}$, $\alpha_2 = 1.80^{+0.18}_{-0.15}$, $t_{\rm break} = 42^{+6.7}_{-7.3}$ ks) with χ^2/d.o.f. = 58.0/44. A 'doubly broken' power law provides a much better statistical fit to the data with χ^2/d.o.f. = 38.7/42 (>99.9 per cent improvement over both the simple and the broken power law). The model consists of a shallow decay, $\alpha_1 = 0.25^{+0.16}_{-0.17}$, which breaks sharply at $t_1 = 7.4^{+1.5}_{-1.5}$ ks to a steeper decay of $\alpha_2 = 1.17^{+0.08}_{-0.09}$. The steeper decay breaks sharply again at $t_2 = 58^{+9.9}_{-15.4}$ ks into a yet more rapidly decaying index of $\alpha_3 = 1.97^{+0.27}_{-0.28}$.

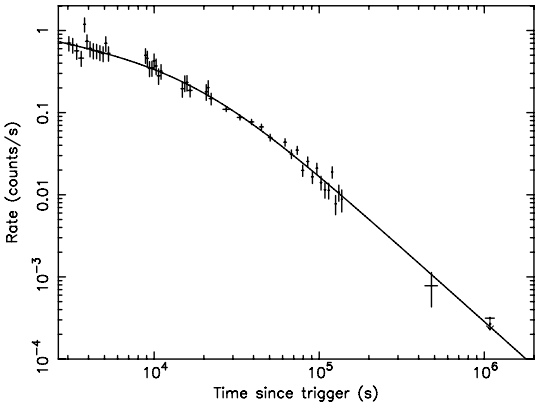

Figure 3. As Fig. 2, but fitted with a smoothly broken power law (see Section 2.1). The first decay slope, $\alpha_1 = 0.37^{+0.13}_{-0.15}$, which breaks at $t = 18.5^{+4.4}_{-3.2}$ ks (observer's frame), with a smoothing parameter $S = 1.0$, to the second decay slope of $\alpha_2 = 1.80^{+0.16}_{-0.16}$.

A 'smoothly broken' power law was also fitted to the data, it consists of two power-law sections; however, the transition between these slopes is not instantaneous, but may spread over several decades in time:

$$f(t) = K \left[\left(\frac{t}{t_{\rm b}} \right)^{-\alpha_1 S} + \left(\frac{t}{t_{\rm b}} \right)^{-\alpha_2 S} \right]^{1/S}, \quad (1)$$

where S is the smoothing parameter, $t_{\rm b}$ is the break time and K is a normalization constant. This produces a smooth break rather than a sharp break as in the previous models. Typically, the values of the smoothing parameter, S, reported in the literature, range between 0.5 and 10, with a value of ∼1 being favoured, both observationally and theoretically (Beuermann et al. 1999; Stanek et al. 2005). A larger value of the smoothing parameter gives a sharper break. The light curve of GRB 050505 is well fitted by a smoothly broken power law with χ^2/d.o.f. ∼1.0. Unfortunately, there is degeneracy between the smoothing factor and the initial decay index, with any value of S between 0.5 and 3 producing a good fit to the data (limit of χ^2/d.o.f. = 1.16). However, if we constrain the model parameters so that α_1 must have a positive value and that α_2 equals p, the electron spectral index (calculated from our spectral index, β, (Zhang & Mészáros 2004)), then we find that a smoothing parameter in the range 0.5–2 is allowed. This range of smoothing factors produces $\alpha_1 \sim 0.5$. Restricting S to 1.0, we find $\alpha_1 = 0.37^{+0.13}_{-0.15}$, $\alpha_2 = 1.80^{+0.16}_{-0.16}$, $t_{\rm break} = 18.5^{+4.4}_{-3.2}$ ks and χ^2/d.o.f.= 46.9/45 (see Fig. 3).

Spectral fits were performed over 0.3–10.0 keV, using grade 0–12 events (as selected for the light curve analysis), binned to 20 counts per data point, individually for co-added data encompassing $T + 3$ to $T + 17$ ks and $T + 26$ to $T + 138$ ks, as well as the summed spectra for both the intervals combined (see Table 1).

The spectra were fitted with a power-law model (see Fig. 4) with the absorption, $N_{\rm H}$, set at the Galactic column density (Dickey & Lockman 1990, 2.1×10^{20} cm^{-2}) and with power-law models with excess absorption (either in our Galaxy or the GRB host galaxy). During our analysis, both the Wisconsin and Tübingen–Boulder ISM absorption models (Arnaud & Dorman 2003) were used; there was no significant difference in either the statistical quality of the fit or in the resulting derived parameters between the two. We present results obtained using the Tübingen–Boulder model using the local ISM abundances of Anders & Grevesse (1989).[4]

It is clear from Table 1 that there is no evidence for spectral change over the duration of the observations. This was confirmed by making a hardness ratio time-series in the bands 0.3–1.5 and 1.5–10.0 keV, no variation was apparent. The fit to the total data set reported in Table 1 also shows that there is significant excess absorption in this spectrum (at >99.99 per cent confidence). Statistically, both the Galactic and extragalactic absorption fits appear equally likely; however, if the excess absorption were to be due to

[4]We also preformed spectral fits, using the abundances of (Wilms, Allen & McCray 2000) and found that they produced $N_{\rm H}$ values that agreed, within errors, to those given by the Anders and Grevesse abundances.

Table 1. Spectral fits for GRB 050505. The spectra show no variation. Whilst an absorbed power law is sufficient to model the data, it can be seen that an additional absorption component proves a better fit, particularly at high redshift.

Model[a]	Co-added data for $T+3$ –$T+17$ ks			Co-added data for $T+26$ –$T+138$ ks			All data co-added		
	Photon index	Excess $N_{\rm H}$ (10^{20} cm^{-2})	χ^2 (d.o.f.)	Photon index	Excess $N_{\rm H}$ (10^{20} cm^{-2})	χ^2 (d.o.f.)	Photon index	Excess $N_{\rm H}$ (10^{20} cm^{-2})	χ^2 (d.o.f.)
PL+Gal	$1.76^{+0.09}_{-0.09}$	–	26.9 (27)	$1.77^{+0.06}_{-0.06}$	–	86.2 (69)	$1.76^{+0.05}_{-0.05}$	–	133 (97)
PL+Gal+Abs	$1.91^{+0.19}_{-0.18}$	<7.74	24.2 (26)	$1.94^{+0.12}_{-0.11}$	$3.91^{+2.43}_{-2.14}$	77.3 (68)	$1.93^{+0.10}_{-0.10}$	$3.81^{+2.09}_{-1.93}$	102 (96)
PL+Gal+ZAbs[b]	$1.87^{+0.15}_{-0.14}$	113^{+123}_{-107}	23.9 (26)	$1.91^{+0.10}_{-0.09}$	133^{+73}_{-65}	74.7 (68)	$1.90^{+0.08}_{-0.08}$	128^{+61}_{-58}	99 (96)

[a]Spectral models: power law (PL), Galactic absorption (Gal), which has been assumed to be 2.1×10^{20} cm^{-2} (Dickey & Lockman 1990), excess Galactic absorption (Abs) and excess absorption in the host galaxy (ZAbs).
[b]z fixed at 4.27.

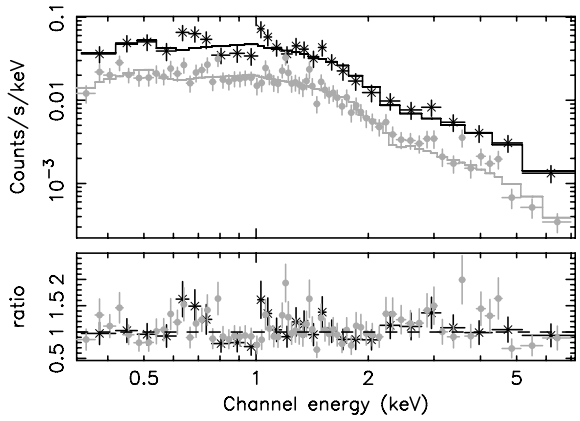

Figure 4. The summed 0.3–10.0 keV spectrum of GRB 050505 from 'piled up' (crosses) and 'non-piled up' (solid circles) data, which are consistent with a photon index of ∼1.90, Galactic absorption (2.1×10^{20} cm^{-2}) plus an excess absorption component from the host galaxy (128×10^{20} cm^{-2}). See Table 1 for a summary of spectral models.

gas in our Galaxy alone, then the value of the excess absorption is almost twice the column density quoted by (Dickey & Lockman 1990). Therefore, we conclude that the bulk component of excess absorption must come from the host galaxy with a value of $N_{\rm H} = 1.28^{+0.61}_{-0.58} \times 10^{22}$ cm^{-2}, assuming local ISM abundances in the GRB rest frame.

The photon index $= \beta + 1 = 1.90^{+0.08}_{-0.08}$, is typical of the photon indices seen in other GRB afterglows (Nousek et al. 2005), even though we are sampling a higher range of spectral energies due to the high redshift of this burst. With a redshift of 4.27 (Berger et al. 2005a), we are measuring the spectrum over a rest-frame range of 1.6–53 keV. The spectrum is well modelled up to such high energies in the rest frame of the GRB, and the photon index is comparable to the values found from low-redshift bursts.

3 FOLLOW-UP DETECTIONS OF GRB 050505.

The first reported detection of an optical counterpart for GRB 050505 was made by Cenko et al. (2005a) observing from the Keck I Telescope, quickly followed by a measurement of the redshift by the same collaboration (Berger et al. 2005a). See Table 2, for a summary of all of the optical observations reported on the Gamma-ray Burst Co-ordination Network (GCN) network, as well as the data from the Faulkes Telescope North, reported here for the first time.

Unfortunately, the initial spacecraft message sent to the GCN network erroneously flagged this event as not a GRB, which consequently meant that the majority of robotic follow-up missions did not observe GRB 050505 promptly. The sparse nature of this combined data set naturally limits the knowledge that can be obtained.

4 DISCUSSION

4.1 Physical origin of the light curve break

A doubly broken power-law fit contains breaks at $7.4^{+1.5}_{-1.5}$ and $58.0^{+9.9}_{-15.4}$ ks in the observer's frame, which translate to $T + 1.4^{+0.3}_{-0.3}$ and $T + 11.0^{+1.9}_{-2.9}$ ks in the rest frame of the burst. The amplitudes of these temporal breaks are $\Delta\alpha_{1-2} = 0.92 \pm 0.19$ and $\Delta\alpha_{2-3} = 0.80 \pm 0.29$.

The combined BAT and XRT light curve (shown in Fig. 5) is consistent with the schematic diagram (fig. 3 of Nousek et al. 2005) of the canonical behaviour of the *Swift* XRT early light curves. For GRB 050505, there is necessarily a steep decline from the bulk of the BAT emission to the early XRT emission, which would comprise the first power-law segment identified by Nousek et al., the early flat slope of the XRT decay (α_1) would comprise the second segment of canonical decay, and the second slope of the doubly broken power-law fit (α_2) would comprise the third canonical segment. The BAT and XRT light curves are consistent with joining in the ∼47 min gap that separates them (see O'Brien et al. 2005), though this behaviour cannot be confirmed with the data available to us.

Light curve breaks can be caused by the passage through the X-ray band of the cooling frequency, the ending of the continued shock energization, the presence of a structured jet or jet deceleration causing the relativistic beaming to become broader than the jet angle. We examine these possibilities here.

We can immediately rule out the presence of a cooling break for either break as this would result in $\Delta\alpha = 0.5$ and a change in spectral index (Sari, Piran & Narayan 1998).

Either of the X-ray light curve breaks might represent the end of the energy injection into the forward shock of the relativistic outflow (Nousek et al. 2005; Zhang et al. 2005, and references therein), given the lack of spectral variation (and presuming the emission before the break was dominated by the forward shock). However, the temporal placement of the first break makes it the more favourable of the two for this interpretation.

Nousek et al. (2005) considered that a shallow flux decay is caused by continuous energy injection into the forward shock either due to a decrease in the Lorentz factor of the outflow towards the end of the prompt emission or by the long-lasting central engine activity. The decreasing Lorentz factor (Γ) scenario requires that $E(>\Gamma) \propto \Gamma^{1-s}$ with $s > 1$, but Nousek et al. found, on the basis of their observed change in decay slope, when modelling the light curve with just a single broken power law, that $s = -16.7 \pm 4.6$ for this burst (see their table 3), thus disallowing this interpretation.

Table 2. Optical follow-up of GRB 050505. Mid-point times are given in seconds after the trigger time.

Filter	Limiting magnitude (mag)	Detected magnitude (mag)	Duration (s)	Mid-point time (s)	Observatory	References
R	9.2		30	0	BOOTES – Very Wide Field Camera	Jelinek et al. (2005)
I		18.2 ± 0.2	456	796	TAROT	Klotz, Boer & Atteia (2005)
I		18.4 ± 0.2	456	1259	TAROT	Klotz et al. (2005)
I	18.8		584	1946	TAROT	Klotz et al. (2005)
R	18.5		1680	2398	AAVSO	Hohman, Henden & Price (2005)
R	19.0		3600	2799	BOOTES – IR	de Ugarte Postigo et al. (2005)
R	19.7		2100	14 326	SARA	Homewood, Hartmann & Wood (2005)
I		20.51 ± 0.05	–	23 006	Keck	Berger et al. (2005b)
g		23.67 ± 0.12	–	23 006	Keck	Berger et al. (2005b)
K		18.1 ± 0.2	–	24 552	UKIRT WFCAM	Rol et al. (2005)
R		21.8 ± 0.1	540	29 894	Faulkes Telescope North	This paper
i'		21.0 ± 0.2	520	30 154	Faulkes Telescope North	This paper
B	21.9		640	30 154	Faulkes Telescope North	This paper

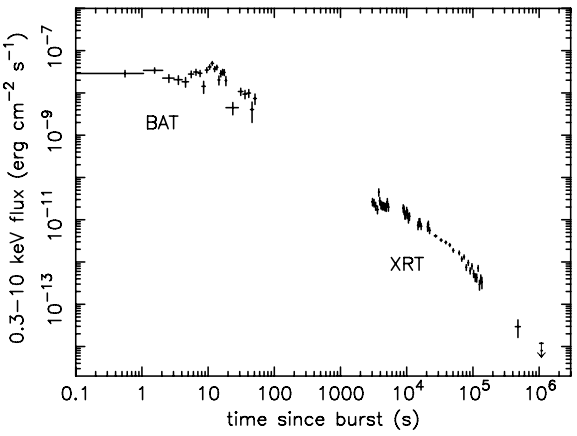

Figure 5. The combined BAT–XRT flux light curve, extrapolated into the 0.3–10.0 keV range. For the XRT section of the flux light curve, the count rate was converted into an unabsorbed flux using the best-fitting power-law model. The BAT data were extrapolated into the XRT band using the best-fitting power-law model derived from the BAT data alone.

However, our more detailed, multibroken power-law analysis shows that this scenario is valid for either of our breaks ($s > 3$ for both the breaks), except when $\nu_c < \nu_x < \nu_m$ for a wind medium ($s \sim -21$ and ~ -63, for the first and second break, respectively).

The long-lasting central engine activity scenario requires that the source luminosity decays slowly with time,[5] $L \propto t_{\rm lab}^{Q}$ with $Q > -1$, with the average value found by Nousek et al. being of the order of -0.5. The change in decay slope from their single broken power-law model leads the authors to find $Q = 0.3 \pm 0.1$ for GRB 050505, which is consistent with the lower limit of this mechanism. However, this value of Q is unphysical as it requires the luminosity to increase with time. Our analysis shows that the long-lasting central engine activity scenario is valid (i.e. $Q < 0$, with Q in the range ~ -0.2 to -0.5), again for either of our breaks, as long as the X-ray frequency, ν_x, is above the cooling frequency, ν_c. We are unable to distinguish, in this case, whether a wind or homogenous cirumburst medium is favoured.

Another possible cause of either of the breaks in the light curve of GRB 050505 could be a structured jet outflow. In this case, the ejecta energy over solid angle, dE/d Ω, is not constant, but varies with the angle θ measured from the outflow symmetry axis (Mészáros 1998). Panaitescu (2005a) suggested that since afterglow light curves are power laws in time, dE/d Ω can be approximated as a power law in θ (see their equation 13), with a power-law index of q.

We assume a typical value of p (the electron spectral index) to be 2.2 (Gallant, Achterberg & Kirk 1999) and use the observed values of $\Delta\alpha$ to calculate q from equations (14) and (15) of Panaitescu (2005a). This relation only applies when $q < \tilde{q}$, where $\tilde{q} = 8/(p+4)$ or $8/(p+3)$. For GRB 050505, the observed values of $\Delta\alpha$ give q greater than $\tilde{q}$, within errors, for both the wind and uniform environments and for the observing frequency above or below the cooling frequency.

For $q > \tilde{q}$, where dE/d Ω falls off sufficiently fast that the afterglow emission is dominated by the core of the jet, we expect $\Delta\alpha = 0.75$ (homogenous environment) or 0.5 (wind environment)

[5] Q in the luminosity relation of Nousek et al. (2005) has been capitalized to prevent confusion with the power-law index q used by Panaitescu (2005a).

(Panaitescu 2005a). Thus, a structured jet appears to be just consistent with both the breaks. However, α_1 is too shallow to be explained by the spherical fireball model, unless the observer is located off the jet core. In this case, the value of α_1 implies that our line of sight should be located exceptionally close to the edge of the core.

The signatures of a jet break, where the relativistic outflow from the GRB slows sufficiently that $\Gamma \sim 1/\theta_j$ and the jet spreads laterally, are a temporal break with a typical amplitude of $\sim$1 (Rhoads 1999; Sari et al. 1999; Chevalier & Li 2000), no spectral variation (Piran 2005) and a post-break decay index equal to p, the electron spectral index (Rhoads 1999). The relation of $\alpha = p$ post-break is valid for $p > 2$, otherwise a different $\alpha - p$ relation should be adopted (Zhang & Mészáros 2004; Dai & Cheng 2001). There is no evidence for spectral variation during our observations (see Table 1). Unfortunately, there were insufficient optical detections of this GRB pre- and post-break to confirm the presence of a jet break in other wavelengths at either epoch.

The temporal index of an X-ray light curve post-jet break should equal p, the electron spectral index (Rhoads 1999). We calculate from our measured spectral index, β, that $p = 1.8 \pm 0.2$ and 2.8 ± 0.3, assuming that ν_x is above and below the cooling frequency, ν_c, respectively (Sari et al. 1999; Zhang & Mészáros 2004). We measure a value of $\alpha_2 = 1.17^{+0.08}_{-0.09}$, which is not compatible with either value of p, which rules out the first break being due to a jet break. However, $\alpha_3 = 1.97^{+0.27}_{-0.28}$ which agrees, within the limits, to the $\nu_x > \nu_c$ case ($p = 1.8 \pm 0.2$). However, since p may be <2, within the error range, we calculated the expected post-break slope from Dai & Cheng (2001; $\alpha = (p + 6)/4$, $\nu_x > \nu_c$) giving an expected decay index of 1.95 ± 0.17, which is also consistent with α_3. With this value of p, we can constrain the jet break parameters further (Rhoads 1999) and conclude that the amplitude of the second break is consistent with a value of 0.95, which is the value expected from optically thin synchrotron emission when $\nu_x > \nu_c$, thus, supporting the case that the second break is a jet break.

Having considered the various potential origins for the breaks in the light curve of GRB 050505 for the doubly broken model, we conclude that the first break is due to the end of energy injection into the forward shock, that is, that GRB 050505 fits with the canonical light curve model proposed by Nousek et al. (2005), and that the second break is due to a jet, either structured or uniform.

The 'smoothly broken' core-dominated power law provides a good fit to the XRT light curve data; however, the large degree of smoothing involved produces a degeneracy between the smoothing parameter, the first decay index and the break time. If we take the example case for $S = 1$ (see Fig. 3), then a break is observed at $T + 18.5^{+4.4}_{-3.2}$ ks in the observer's frame. This translates to $T + 3.5^{+0.8}_{-0.6}$ ks in the rest frame of the burst, with $\Delta\alpha = 1.43^{+0.21}_{-0.22}$.

The magnitude of this break allows us to rule out a cooling break or the end of continued energy injection into the forward shock. A structured jet could explain the magnitude of this break if the observer is placed off the jet core (Panaitescu 2005b). This would then naturally explain the initial shallow decay index and the very smooth break. The magnitude of the break is also compatible with a jet break from optically thick synchrotron emission ($\Delta\alpha = 1.25$). However, a break this early requires an unreasonably large circumburst density ($n \sim 3 \times 10^5$ cm^{-3}) to produce a value of $E_{\gamma,\rm rest}$ (Ghirlanda et al. 2004), the true γ-ray energy released, that is comparable with the typical values of $E_{\gamma,\rm rest}$ seen thus far (Bloom, Frail & Kulkarni 2003). Thus, the parameters of the smoothly broken power-law model fit are inconsistent with all of the afterglow models considered here.

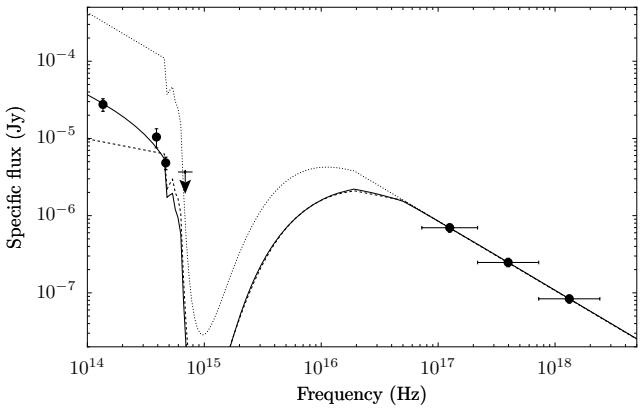

Figure 6. The optical–near-infrared (optical–NIR) to X-ray spectrum of GRB 050505 at 32 ks after the burst. The X-ray fluxes are corrected for both the Galactic and host-galaxy absorption, while the optical–NIR points have been corrected for Galactic absorption only. The optical *R*-band point lies on the edge of the Lyman break, with the Gunn–Peterson trough bluewards of it. The continuous line represents a broken power law, modified by the Lyman break and additional optical–UV host-galaxy extinction (see text). The dashed line uses the same model, but with no additional extinction. The dotted line is the extrapolation from a single power law fitted to the X-rays alone, only accounting for the Lyman break.

4.2 Multiwavelength spectral energy distribution

In Fig. 6, we show the optical–X-ray spectrum of GRB 050505. The X-ray fluxes were obtained from a spectral fit between 26 and 40 ks, after the bursts; the optical data [the United Kingdom Infrared Telescope (UKIRT) *K*-band and the FTN data] were scaled to a common epoch, chosen to be the logarithmic average of the X-ray data (32 ks). The magnitudes have been corrected for the estimated Galactic extinction, using the dust maps by Schlegel, Finkbeiner & Finkbeiner (1998), and have been converted to fluxes using the calibration provided by Fukugita, Shimasaku & Ichikawa (1995) for the optical and that by Tokunaga & Vacca (2005) for the infrared magnitudes. Since all the optical data were taken between the time of the two breaks, we have used the $\alpha_2 = 1.17$ light curve decay index. However, the decay in the optical can be different. We tested several other values for the decay index (at most 0.5 different from 1.17), and found the resulting optical fluxes differ at most by 1σ ($\sim$0.2 mag).

We fit the broad-band spectrum with two basic models, a power law and a broken power law, both accounting for the Lyman break (with the redshift fixed at $z = 4.27$) and intrinsic host-galaxy extinction (also with the redshift fixed at $z = 4.27$). The Lyman break has been modelled as described in Madau (1995); the optical–ultraviolet (optical–UV) absorption has been modelled following Pei (1992). A single power law is excluded, even allowing for dramatic extinction in the host galaxy (χ^2/d.o.f.=38.19/4 with the spectral index fixed at 0.9 as determined from the X-ray data alone). A broken power law, with the high-frequency index β_2 also fixed at 0.9, results in a much better fit. We have applied three variants of extinction: none, a Galactic-like extinction curve and a Small Magellanic Cloud like (SMC-like) extinction curve. The SMC-like extinction curve provides a good fit, resulting in the $B - V$ colour excess being $E(B - V) = 0.10 \pm 0.02$ and the low-frequency index $\beta_1 = 0.41^{+0.05}_{-0.06}$ (1σ confidence limits). The break frequency is largely unrestricted and was kept fixed at a value of 10^{16} Hz, although values of 10^{17} and 10^{15} Hz are acceptable (with varying amounts of host-galaxy extinction). However, the low number of data points results in a relatively

low χ^2/d.o.f.$\sim$0.3, and shows a certain degeneracy: a Galactic-like extinction curve results in an equally good fit. This is mostly because the observed wavelength of the distinct 2175-Å feature[6] falls between our available photometry at this redshift, and the intrinsic extinction is almost entirely determined from the two *K*- and *I*-band points (the *R*-band point being located on the edge of the Lyman break). The resulting values for a Galactic extinction curve are $E(B-V) = 0.20 \pm 0.03$ and $\beta_1 = 0.50^{+0.06}_{-0.07}$ (1σ).

The difference between the two power-law indices is $\Delta\beta \sim 0.5$. To obtain a better constraint for the break frequency, we have fixed the indices at $\beta_1 = 0.4$ and $\beta_2 = 0.9$. This results in the cooling frequency being located between 1.8×10^{15} and 1.4×10^{16} Hz (this is dependent on whether a Galactic or an SMC extinction curve is used). The inferred $E(B-V)$ is the same as before.

Our best-fitting results favour a cooling break between the optical and X-ray wavebands; in addition, a modest amount of host-galaxy extinction would be needed to explain our data fully, but no clear distinction between the Galactic and SMC-like extinction can be made. A fit with an SMC-like extinction, however, agrees marginally better with the expected $\Delta\beta = 0.5$ for a cooling break.

Berger et al. (2005b) measured a hydrogen column density of log $N_{\rm H\,I} = 22.05 \pm 0.10$ from the Lyman α(Lyα) absorption in their optical spectrum, and a metallicity of $Z \approx 0.06\,Z_{\odot}$. We can therefore immediately rule out the Galactic like extinction. Fitting the X-ray spectrum with intrinsic absorption, setting all elements heavier than He to an abundance of 0.06, gives $N_{\rm H} = 7.43^{+3.77}_{-3.41} \times 10^{22}$ cm^{-2}, that is, log $N_{\rm H} = 22.87^{+0.18}_{-0.27}$, in addition to the Galactic absorption component. This host absorption is higher than the hydrogen column directly measured by Berger et al. (2005b). It is unlikely that this difference is caused by an evolution of the dust and gas properties, since the time-scales of the X-ray and optical observations are similar. A reconciliation of these results can, in principle, be achieved by ionization in the host; however, the ionization fraction required is too high as to be considered seriously.

The magnitude of the difference between these two hydrogen column densities is not easily explained. We estimate a 10 per cent error in the Galactic $N_{\rm H}$ in this direction. Setting the Galactic column density to 110 per cent of its value does not reduce the excess hydrogen column density in the rest frame of the burst sufficiently to reconcile the X-ray absorption with the value of Berger et al. (2005b). Nor can a difference in column densities of this magnitude be explained by the remaining uncertainties in the XRT calibration.

We also performed a spectral fit allowing both Galactic and host values of $N_{\rm H}$ to vary, rather than constraining the Galactic value to that given by Dickey & Lockman (1990), using the XSPEC STEPPAR command to explore the absorption column parameter space. The host absorption column still exceeded the value given by Berger et al. (2005b) at greater than 90 per cent confidence. We speculate that some curvature of unknown origin may be present in the X-ray spectrum.

From the hydrogen column density, and using the relation between $N_{\rm H\,I}$ and $E(B-V)$ for the SMC (Martin, Maurice & Lequeux 1989), we can infer $E(B-V) = 0.24$. We note that this value is likely to be lower, with the metallicity being half of the estimated SMC ISM metallicity (Pei 1992). The inferred value is moderately in agreement with the $E(B-V) = 0.10$ we find from directly fitting the optical–X-ray spectrum with an SMC-like extinction curve (assuming $R_V = 2.93$), although the Galactic extinction curve results in an extinction measurement which is equally well compatible with the inferred $E(B-V)$. This approximately agrees with $A_V = R_V \times E(B-V) = 0.3$ as found by Berger et al. (2005b). Such a low extinction value is not uncommonly seen in the GRB afterglows (e.g. Galama & Wijers 2001; Stratta et al. 2004).

[6]A strong increase in absorption is found for both the Milky Way and Large Magellanic Cloud around this wavelength, but is notably absent in the SMC (see e.g. Savage & Mathis 1979).

4.3 Burst properties

From the redshift of GRB 050505 ($z = 4.27$) and the mean flux over the observed 15–350 keV T_{90} spectrum, we calculate an isotropic equivalent radiated energy, $E_{\rm iso,rest}$, in the extrapolated 1–10^4 keV rest-frame energy range to be $4.44^{+0.80}_{-1.12} \times 10^{53}$ erg, using the standard cosmology (Spergel et al. 2003): $H_0 = 71$ km s^{-1} Mpc^{-1}, $(\Omega_{\rm M}, \Omega_{\Lambda}) = (0.27, 0.73)$, and a *K*-correction of $3.09^{+0.48}_{-0.33}$.

If we take the second break in the light curve to be a jet break, we are then able to calculate the properties of GRB 050505. Using the formulation of Frail (2001), and assuming that the efficiency of the fireball in converting the energy of the ejecta into γ-rays is $\sim$0.2, we obtain a range in θ_j from $2\overset{\circ}{.}2 (n = 1 {\rm cm}^{-3})$ to $3\overset{\circ}{.}8 (n = 100\ {\rm cm}^{-3})$ (Panaitescu & Kumar 2002). Frail (2001) concluded that opening angles of $\leqslant 3^{\circ}$ are required for less than 10 per cent of the *BeppoSAX* GRB sample. However, such a narrow beaming angle would not be unexpected for a high-redshift burst as GRBs with wide jets would be too faint to be detected by current γ-ray missions.

From this we can calculate the beaming fraction $f_{\rm b} = (1 - \cos\theta_j)$ (Sari et al. 1999) to be between 7.1×10^{-4} ($n = 1$ cm^{-3}) and 2.3×10^{-3} ($n = 100$ cm^{-3}) and $E_{\gamma,\rm rest}$, the true γ-ray energy released, to be in the range of $3.17^{+0.86}_{-1.11} \times 10^{50}$ ($n = 1$ cm^{-3}) to $9.99^{+3.00}_{-3.24} \times 10^{50}$ erg ($n = 100$ cm^{-3}) for a rest-frame energy band of 1–10^4 keV. We note that the typical $E_{\gamma,\rm rest}$ of bursts, thus far, is 9.8×10^{50} erg (Bloom et al. 2003) with a burst-to-burst variance about this value of $\sim$0.35 dex (or a factor of 2.2); thus, this burst agrees well with the typical value, provided the circumburst density is of the order of 100 cm^{-3}.

We found it useful to calculate $E_{\rm peak,rest}$ from these values of $E_{\gamma,\rm rest}$ via the Ghirlanda relation (Ghirlanda, Ghisellini & Lazzati 2004) and compare these values to the observed lower limit of $E_{\rm peak,obs} > 52$ keV ($E_{\rm peak,rest} > 274$ keV). We calculated that the Ghirlanda relation gave $E_{\rm peak,rest} = 215^{+39}_{-51}$ (for $n = 1$ cm^{-3}) and 484^{+130}_{-125} keV (for $n = 100$ cm^{-3}), which agrees with the lower observed limit if the circumburst density is high. We also calculated $E_{\rm peak,rest}$ via the Amati correlation (Amati et al. 2002; Lloyd-Ronning & Ramirez-Ruiz 2002). Using equation (6) of Ghirlanda, Ghisellini & Firmani (2005) for GRBs of known redshift gives $E_{\rm peak,rest} = 1000^{+115}_{-151}$ keV, consistent with our observed limit.

5 CONCLUSIONS

We have presented multiwavelength data for GRB 050505. Our earliest X-ray data start $\sim$47 min after the GRB trigger time as the *Swift* satellite was unable to slew to it immediately due to an Earth limb constraint. The X-ray light curve of GRB 050505 (see Figs 2 and 3) can be adequately fitted with either a 'smoothly broken' or 'doubly broken' power-law model.

The 'smoothly broken' power-law model (see Fig. 3) favours a smoothing factor of 0.5–2 (highly smoothed transition). This produces an initially shallow decay with $\alpha_1 \sim 0.5$, which breaks over several decades in time to a steeper slope, α_2, of $\sim$1.8 (χ^2/d.o.f. $\sim$1.04). The values of the decay indices are poorly constrained but, assuming a smoothing parameter $S = 1$, then a break is observed at $T + 18.5^{+4.4}_{-3.2}$ ks in the observer's frame with

$\Delta\alpha = 1.43^{+0.21}_{-0.22}$. The magnitude of this break is inconsistent with all of the afterglow models considered here.

A 'doubly broken' power-law model (see Fig. 2) consists of a shallow decay, $\alpha_1 = 0.25^{+0.16}_{-0.17}$, first detected at $T + 3$ ks, followed by a break in the observer's frame at $t_1 = 7.4^{+1.5}_{-1.5}$ ks and a steeper decay $\alpha_2 = 1.17^{+0.08}_{-0.09}$. This decay breaks sharply again at $t_2 = 58^{+9.9}_{-15.4}$ ks into a yet more rapidly decaying index of $\alpha_3 = 1.97^{+0.27}_{-0.28}$, which continues until at least $T + \sim$500 ks (χ^2/d.o.f.= 38.7/42).

We see no change in the X-ray spectral properties during *Swift*'s observations of this GRB. The best-fitting model parameters for the X-ray spectrum indicate that this burst has a typical photon index of $1.90^{+0.08}_{-0.08}$ and an excess absorption component from the host galaxy of $(1.28^{+0.61}_{-0.58}) \times 10^{22}$ cm^{-2} (χ^2/d.o.f.= 99/96).

Having considered the temporal position and amplitude of the two breaks in the doubly broken light curve, we conclude that the first break is due to the end of energy injection into the forward shock (Nousek et al. 2005; Zhang et al. 2005), that is, that GRB 050505 fits with the canonical light curve model proposed by Nousek et al. (2005), and that the second break is jet break caused by either a structured or uniform jet.

The optical–X-ray spectrum indicates that the cooling break is located between the optical and X-ray bands, as seen in many other GRB afterglows. A modest amount of intrinsic optical–UV extinction is required in addition, which for an SMC-like extinction law would result in $E(B - V) = 0.10$. We note that a Galactic extinction law fits equally well, but the value of $0.06\,Z_\odot$ inferred from the optical spectrum (Berger et al. 2005b) shows it to be more SMC-like. Interestingly, the N_H column density inferred from the X-ray spectrum with the metallicity set to $0.06\,Z_\odot$ is higher than that directly measured from the H I column.

The redshift of 4.27 allowed us to calculate the intrinsic parameters for this GRB, in conjunction with the second light curve break time observed in *Swift*'s X-ray observations. The identification of this break with a jet break provides a value for $E_{\gamma,\mathrm{rest}}$ that is in good agreement with respect to previous GRBs, provided that the circumburst density is of the order of 100 cm^{-3} and the values are consistent with the Ghirlanda (Ghirlanda et al. 2004, 2005) and Amati (Amati et al. 2002; Lloyd-Ronning & Ramirez-Ruiz 2002) relations. It also suggests that GRB 050505 has a narrow beaming angle; however, this degree of beaming is not unexpected for GRBs at high redshift, since GRBs with wider jets could potentially be too faint to be detected by any of the current γ-ray missions.

ACKNOWLEDGMENTS

This work is supported at the University of Leicester by the Particle Physics and Astronomy Research Council (PPARC) and at Penn State by NASA contract NAS5-00136. The Faulkes Telescope North is supported by the Dill Faulkes Educational Trust. CPH gratefully acknowledges support from a PPARC studentship. VLP, MP and PR gratefully acknowledge ASI grant I/R/039/04. The authors acknowledge Iain Steele (LJMU) and Cristiano Guidorzi (LJMU) for their assistance with the FTN observations and Rhaana Starling (University of Amsterdam) for useful discussions. We are also grateful to the referee, Bruce Gendre, for his constructive and valuable comments.

REFERENCES

Amati L. et al., 2002, A&A, 390, 81.
Anders E., Grevesse N., 1989, Geochimica et Cosmochimica Acta., 53, 197
Andersen M. I. et al., 2000, A&A, 364, L54
Arnaud K., Dorman B., 2003, XSPEC online manual
Barthelmy S. D. et al., 2005, Space Sci. Rev., 120, 143
Berger E., Cenko S. B., Steidel C. C., Reddy N., Fox D. B., 2005a, GCN Circ., 3368
Berger E., Penprase B. E., Cenko S. B., Kulkarni S. R., Fox D. B., Steidel C. C., Reddy N., 2005b, ApJ, submitted (astro-ph/0511498)
Beuermann K. et al., 1999, A&A, 352, L26
Bloom J. S., Frail D. A., Kulkarni S. R., 2003, ApJ, 594, 674
Burrows D. N. et al., 2005, Space Sci. Rev., 120, 165
Cenko S. B., Steidel C. C., Reddy N., Fox D. B., 2005a, GCN Circ., 3366
Cenko S. B., Steidel C. C., Reddy N., Fox D. B., 2005b, GCN Circ., 3377
Chevalier R. A., Li Z., 2000, ApJ, 536, 195
Cusumano G. et al., 2005, Nat, submitted (astro-ph/0509737)
Dai Z. G., Cheng K. S., 2001, ApJ, 558, L109
Dickey J. M., Lockman F. J., 1990, ARA&A, 28, 215
Frail D. A., 2001, ApJ, 562, L55
Fruchter A., Krolik J. H., Rhoads J. E., 2001, ApJ, 563, 597
Fukugita M., Shimasaku K., Ichikawa T., 1995, PASP, 107, 945
Galama T. J., Wijers R. A. M. J., 2001, ApJ, 549, L209
Gallant Y., Achterberg A., Kirk J. G., 1999, A&AS, 138, 549
Gehrels N. et al., 2004, ApJ, 611, 1005
Ghirlanda G., Ghisellini G., Lazzati D., 2004, ApJ, 616, 331
Ghirlanda G., Ghisellini G., Firmani C., 2005, MNRAS, 361, L10
Grazian A. et al., 2006, GCN Circ., 4545
Hjorth J. et al., 2003, Nat, 423, 847
Hohman D., Henden A., Price A., 2005, GCN Circ., 3370
Homewood A., Hartmann D. H., Wood M., 2005, GCN Circ., 3398
Hullinger D. et al., 2005, GCN Circ., 3364
Hurkett C. P. et al., 2005, GCN Circ., 3360
Jelínek M., Castro-Tirado A. J., Gorosabel J., de Ugarte Postigo A., Guziy S., Kubanek P., Hudec R., Vitek S., 2005, GCN Circ., 3373
Kawai N., Yamada T., Kosugi G., Hattori T., Aoki K., 2005, GCN Circ., 3937
Kennea J. A., Burrows D. N., Hurkett C. P., Osborne J. P., Gehrels N., 2005, GCN Circ, 3365
Kippen R. M., 2000, GCN Circ., 530
Klotz A., Boer M., Atteia J. L., 2005, GCN Circ., 3403
Lamb D. Q., Reichart D. E., 2000, ApJ, 536, 1
Lloyd-Ronning N. M., Ramirez-Ruiz E., 2002, ApJ, 576, 101
Madau P., 1995, ApJ, 441, 18
Malesani D. et al., 2006, GCN Circ., 4541
Martin N., Maurice E., Lequeux J., 1989, A&A, 215, 219
Mészáros P., Rees M. J., Wijers R., 1998, ApJ, 499, 301
Moretti A. et al., 2005, A&A, 448, 49
Nousek J. A. et. al., 2005, ApJ, in press (astro-ph/0508332)
O'Brien P. T. et al., 2005, ApJ, submitted (astro-ph/0601125)
Panaitescu A., Kumar P., 2002, ApJ, 571, 779
Panaitescu A., 2005a, MNRAS, 362, 921
Panaitescu A., 2005b, MNRAS, 363, 1409
Pei Y. C., 1992, ApJ, 395, 130
Piran T., 2005, Rev. Mod. Phys. 76, 1143
Rhoads J. E., 1999, ApJ, 525, 737
Rol E., Tanvir N., Levan A., Adamson A., Fuhrman L., Priddey R., Chapman R., 2005, GCN Circ., 3372
Roming P. W. A. et al., 2005, Space Sci. Rev., 120, 95
Rosen S., Hurkett C., Landsman W., Roming P., Poole T., Gehrels N., Mason K., Nousek J., 2005, GCN Circ., 3367
Rosen S., Hurkett C., Holland S., Roming P., Blustin A., Gehrels N., Mason K., Nousek J., 2005, GCN Circ., 3371
Sari R., Piran T., Narayan R., 1998, ApJ, 497, L17
Sari R., Piran T., Halpern J. P., 1999, ApJ, 519, L17
Savage B. D., Mathis J. S., 1979, ARA&A, 17, 73
Schlegel D. J., Finkbeiner D. P., Davis M., 1998, ApJ, 500, 525
Spergel et al., 2003, ApJS, 148, 175
Stanek K. Z. et al., 2003, ApJ, 591, L17
Stanek K. Z. et al., 2005, ApJ, 626, L5
Stratta G., Fiore F., Antonelli L. A., Piro L., De Pasquale M., 2004, ApJ, 608, 846

Tagliaferri G. et al., 2005, A&A, 443, L1
Tinney C. et al., 1998, IAU Circ., 6896
Tokunaga A. T., Vacca W. D., 2005, PASP, 117, 421
de Ugarte Postigo A. et al., 2005, GCN Circ., 3376
Vaughan S. et al., 2006, ApJ, 638, 920
Vreeswijk P. M. et al., 2004, A&A, 419, 927
Watson D. et al., 2006, ApJ, 637, L69
Wilms J., Allen A., McCray R., 2000, ApJ, 542, 914
Zhang B., Mészáros P., 2004, IJMPA, 19, 2385
Zhang B., Fan Y. Z., Dyks J., Kobayashi S., Meszaros P., Burrows D. N., Nousek J. A., Gehrels N., 2006, ApJ, in press (astro-ph/0508321)

This paper has been typeset from a TEX/LATEX file prepared by the author.